COBEM 99
XV Congresso Brasileiro de Engenharia Mecânica
15th Brazilian Congress of Mechanical Engineering
22 - 26 de Novembro de 1999 / November 22 - 26, 1999 Águas de Lindóia, São Paulo,

DETERMINATION OF THE VIBRATION CHARACTERISTICS OF NUCLEAR FUEL RODS IN A FLUID FLOW USING MULTIPHYSICS COMPUTATION

Ricardo Sbragio
Centro Tecnológico da Marinha em São Paulo
Av. Prof. Lineu Prestes 2242, Cidade Universitária, SP, Brasil

Abstract. *The determination of natural frequencies and displacement Power Spectrum Density (PSD) of fuel rods in a fluid using Computational Fluid Dynamics (CFD) and Finite Element Methods (FEM) is presented. The rods are modeled as slender beams subjected to small displacements in a fluid using three-dimensional mesh. The incompressible Navier-Stokes and linear momentum balance equations are solved simultaneously using Spectrum code. Two examples from literature are analyzed. The first consists in one rod in a fluid. The excitation is an impulse force at the rod central node. The second example is a two rod system in a fluid. In this case, the excitation force is random and is determined from a PSD.*

Key words: *Vibrations, CFD, Nuclear Fuel Rods*

1. INTRODUCTION

Nuclear fuel rods are subjected to turbulent axial flow that induce lateral vibrations. These vibrations can cause failures of the fuel rods if their movements exceed a reasonable value, with the possibility of releasing nuclear material and consequent shutdown of the plant.

The flow around the rods is eminently axial. The random turbulence of this flow alters the velocity field on the rods and consequently the pressure field. Hence, random excitation is generated provoking rod vibrations. In previous works, the usual approach to analyze random vibrations was to apply the excitation PSD into the transfer function of the system in order to obtain the rod displacement PSD. This paper presents another method to calculate the natural frequencies and displacement PSD of the rods by using multiphysics analysis in a FEM/CFD solver. The solver used is the Spectrum, developed by Centric Engineering Systems Inc. This code was chosen because of its capacity of solving the fluid flow and rod structural problem simultaneously. This method has the advantage of considering the three-dimensionality of the fluid-rod interaction problem but it requires considerable computer resources.

Two examples are presented. The first determines the natural frequencies of a rod in a fluid and was experimentally studied by Burgreen *et al.* (1958). The excitation force is a unit impulse applied at the rod central node. The second example determines the natural frequencies and PSD of a two rod system in a fluid, and was analytically studied by Païdoussis *et al.* (1985). A random excitation obtained from samplings of a force PSD is input at the rods.

2. GENERAL MODEL OF THE FLUID-ROD SYSTEM

The simulation of rod vibrations in a fluid is done using Spectrum code by solving numerically the linear momentum balance and the Navier-Stokes equations. The relevant numerical schemes used in this code are briefly presented in this Section.

The system consists of the rods and the turbulent axial flow. The domain is divided in three parts. The first is the rod solid domain which is modeled using a linear stress analysis equation with small deformations. The second part is the fluid domain, modeled by an isothermal incompressible Navier-Stokes equation. Both the solid and fluid meshes are composed of three-dimensional eight-noded elements. The third part is the fluid-solid interface, composed of two-dimensional four-noded elements. The interface nodes belong to both solid and fluid regions.

The fluid uses the Arbitrary Lagrangian Eulerian (ALE) mesh concept (Centric, 1993). This concept analyzes the fluid by the Eulerian viewpoint when it flows through the mesh and by the Lagrangian viewpoint when mesh deformations are considered. In fluid problems with fixed boundaries, the Eulerian viewpoint is used as it is impossible to follow fluid particles. The main interest is in the domain which is fixed in time. However, for problems with changes in the boundary, like the fluid-solid interaction problem, it is necessary to allow mesh movements and the Eulerian viewpoint is difficult to use. For the cases where the domain needs to move, the Lagrangian viewpoint is better, as it follows particles in time. The ALE model is designed to allow mesh movements. In this model, the fluid flows through a moving mesh. Thus, the model is a hybrid between the Eulerian and Lagrangian viewpoints, updating the nodal coordinates and field variables in response to the moving boundaries while mesh connectivity is maintained.

3. METHOD OF ANALYSIS OF ROD MOVEMENTS IN FREQUENCY DOMAIN

The frequency domain analysis determines the displacement PSD and natural frequencies and consists of two parts: the first is a pre-processing part where the force PSD and variance are determined. The time dependent forces are sampled using a Monte Carlo procedure and applied into the FEM/CFD model. The second part is the post-processing which determines the rod displacement PSD. This analysis is used in the two-rod-fluid system of Section 5.

3.1 Preprocessing part: Determination of force excitation and sampling procedure

The determination of the pressure Cross Spectral Density (CSD) and PSD on the rods is a complicated task that can be done by experimental measurements of the pressure field. From the pressure CSD and PSD, the force CSD and PSD in the *x* and *y* directions are obtained by:

$$S_{f_x f_x}(z,z',\omega) = R^2 \int_0^{2\pi} d\theta \int_0^{2\pi} d\theta' S_{pp'}(z,z',\theta,\theta',\omega)\cos\theta\cos\theta', \tag{1}$$

$$S_{f_x f_y}(z,z',\omega) = R^2 \int_0^{2\pi} d\theta \int_0^{2\pi} d\theta' S_{pp'}(z,z',\theta,\theta',\omega)\cos\theta\sin\theta', \text{ and} \tag{2}$$

$$S_{f_y f_y}(z,z',\omega) = R^2 \int_0^{2\pi} d\theta \int_0^{2\pi} d\theta' S_{pp'}(z,z',\theta,\theta',\omega)\sin\theta\sin\theta'. \tag{3}$$

where θ and θ' are the angular positions where pressures are measured, z and z' are the axial positions and ω is the circular frequency. Next, the resulting force PSD and CSD are

used to determine the auto- and cross-correlations of the force distribution. These correlations are represented by $R_{f_i f_j'}(z,z',\tau)$ (subscripts *i* and *j* can be *x* or *y*) and are given by:

$$R_{f_i f_j'}(z,z',\tau) = \frac{1}{2\pi}\int_{-\infty}^{\infty} S_{f_i f_j'}(z,z',\omega)\exp(i\omega\tau)d\omega\,, \text{ or} \tag{4}$$

$$R_{f_i f_j}(z,z',\tau) = \frac{1}{\pi}\int_{0}^{\infty} S_{f_i f_j}(z,z',\omega)\cos(\omega\tau)d\omega\,, \tag{5}$$

as the PSD and CSD are even functions. The correlation $R_{f_i f_j'}(z,z',\tau)$ is used to determine the variance and covariance of the fluctuating force distribution for any position pair (z,z') and for any time interval τ. The process is considered stationary. Hence, the covariance values are the same for any equal time interval τ. The fluctuating force distribution is assumed to follow a multidimensional Gaussian probability density function (*pdf*) with zero mean. The covariance of the force *pdf* for two axial positions z,z' and for a time interval τ is:

$$\mathrm{cov}\left[f_i(t), f_j(t+\tau)\right] = E\left[f_i(t)f_j(t+\tau)\right] - E\left[f_i(t)\right]E\left[f_j(t+\tau)\right] = E\left[f_i(t)f_j(t+\tau)\right] = R_{f_i f_j}(z,z',\tau)\ . \tag{6}$$

With the variance and covariance of the force *pdf* known, the fluctuating force at each rod central node is sampled as a function of time using a Monte Carlo code and input in the rods.

3.2 Postprocessing part: Determination of displacement PSD and natural frequencies

The output of the Spectrum solver is the rod displacement as a function of time. From this output, the displacement PSD of the rod is determined and the natural frequencies obtained from the peaks of the PSD curve. Two input parameters of the FEM code that influence this solution must be analyzed: the total run time of the solver and the maximum time step.

- Total run time of the FEM solver: The total run time can be determined from the desired frequency scale resolution of the solution displacement PSD graph (Fig.1). This resolution must allow the determination of the natural frequency differences of the modes of vibration. This can be verified using the Fourier series expression. For a vector *x* (displacement) that represents a length *N* discrete signal obtained at time *t* with time step *dt*, the Fourier series is:

$$x(n) = a_0 + \sum_{k=1}^{N/2} a_k \cos\left(\frac{2\pi k}{Ndt}t(n)\right) + \sum_{k=1}^{N/2} b_k \sin\left(\frac{2\pi k}{Ndt}t(n)\right). \tag{7}$$

The frequency resolution of the displacement PSD is obtained by setting *k=1* in Eq. (7), resulting in $2\pi/(Ndt)$ rad/s or $1/(Ndt)$ Hz. As *Ndt* is the total run time for the program, we have that the desired frequency resolution determines the total run time of the solver.

- Maximum time step for the FEM solver: The maximum time step *dt* used in the FEM solver for the rod displacement determination is given by the maximum frequency that is desired to be obtained in the frequency scale of the displacement PSD graph. This maximum frequency must be larger than the natural frequency of the system. From Eq. (7), the maximum frequency of the displacement PSD graph is obtained when *k=N/2*, which is π/dt rad/s or $1/(2dt)$ Hz.

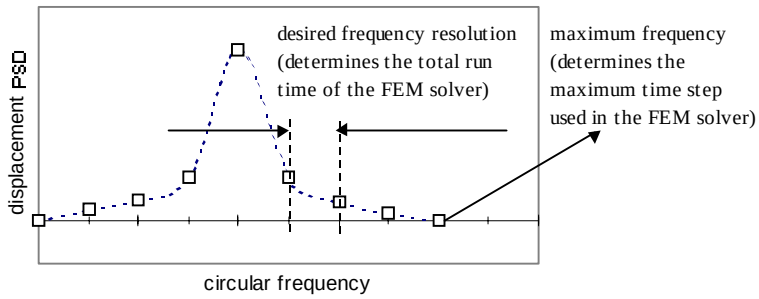

Figure 1 - Definition of FEM solver parameters: total run time and maximum time step

4. EXAMPLE 1: NATURAL FREQUENCY OF A ROD IN A FLUID

The first example determines the fundamental natural frequency of a rod in a fluid. The rod in this analysis corresponds to case *C* of Burgreen *et al.* (1958). The authors presented experimental results for the natural frequency of a single rod and for a bundle of rods as a function of the mean flow velocity. The rod is simply supported. The inlet flow profile is modeled by a power law, as shown in Eq. (8). This equation considers the flow in the *z-axis* direction inside a pipe of radius *R*. The value of exponent *n* is a function of Reynolds number and was measured by Nikuradse (Hinze, 1975). For Reynolds numbers correspondent to the flow velocities of Table 1, the value of *n* is about 8.

$$V_z(r)/V_{z\max} = (1 - r/R)^{1/n} \quad . \tag{8}$$

4.1 Analytical value for the natural frequency of a rod in vacuum

The fundamental natural frequency for a simply supported rod in vacuum is given by Eq. (9). For the aluminum rod (see data in Table 1), the fundamental natural frequency in vacuum is 130.28 rad/s (20.7 Hz). Burgreen's measurement for this natural frequency was 20 Hz.

$$\omega_1 = \frac{\pi^2}{L^2}\left(\frac{EI}{\rho A}\right)^{1/2} \quad . \tag{9}$$

Table 1. Characteristics of the aluminum rod, channel and fluid (Burgreen *et al.*, 1958)

rod density ρ	0.1 lb/in^3
rod diameter d	0.625 in
rod area A	0.3068 in^2
rod length L	48.0 in
rod inertia I	7.350e-3 in^4
Young's module E	10e6 psi
Hydraulic diameter	0.470 ft
Channel diameter	6.25 in
Channel length	72 in
fluid density	62.205 lb/ft^3
fluid viscosity	6.412e-4 lb/(ft s)
fluid mean velocities used in the model	0, 6.2, 8.6, 12.2, 13.5, and 15.0 ft/s

4.2 FEM determination of the natural frequency of the rod in vacuum

The natural frequency of the rod in vacuum was determined using Spectrum code in order to verify the mesh refinement. The rod mesh has 279 nodes and 120 elements (30 longitudinal divisions). The natural frequency obtained from Spectrum code is 20.91 Hz. The run time was about 20s on an HP-UX workstation. The result was considered satisfactory and this mesh was used in the next step, which is the determination of the natural frequencies of the rod in a fluid.

4.3 FEM/CFD determination of the natural frequency of the rod in a fluid

The rod mesh is the same used in Section 4.2. The fluid mesh has 1784 nodes and 1464 elements. Its cross section is shown in Fig. 2. The fluid-rod interface has 248 four-noded plane elements. The fluid region is 1.5 times the length of the rod region, with the rod centered in it. The inlet fluid region length is divided into three parts. The mean fluid region length is divided into thirty parts, following the rod division. The outlet fluid region length is divided into two parts. For the cases where flow velocity is not zero, a previous CFD problem was run in order to determine velocity and pressure in each fluid node, with the following boundary conditions: all rod nodes are restrained, zero flow velocity at channel wall, non slip condition at fluid-rod interface, inflow velocity given by a power-law profile with mean values given in Table 1, no displacement of the fluid mesh at channel wall, and zero pressure at the outflow.

The fluid velocity and pressure results of this CFD problem were used in the fluid-rod interaction problem as initial condition. For the fluid-rod interaction problem, the boundary conditions are the same as mentioned above, except for the first one as rod displacements are allowed. For this case, the first boundary condition states that the rod is simply supported, being the others boundary conditions the same. The excitation force is a unit impulse with 0.01s of duration applied at the rod central node at time zero.

The results are compared to the results of Burgreen *et al.* (1958) in Table 2. In this table, the results of a previous simulation using 10 longitudinal divisions in the rod are also presented in order to show how mesh refinement influences the results. The run time for each natural frequency determination, involving 2 to 3 periods of the harmonic movement of the rod central node, was about 25 hours on an HP-UX workstation (for the 30 longitudinal division case).

Table 2. Results from FEM/CFD model and from rod #2 of Burgreen *et al.* (1958).

fluid velocity (ft/s)	results for 10 divisions in the rod length (Hz)	results for 30 divisions in the rod length (Hz)	results from Burgreen (Hz)
no fluid (in vacuum)	21.48	20.91	20
0 (static water)	17.93	17.38	17
6.2	18.59	18.14	17.5
8.6	18.33	18.07	17.5
10.6	18.30	18.02	17.5
12.2	18.51	17.98	17.5
13.5	18.30	17.90	17.5
15.0	18.33	17.94	17.5

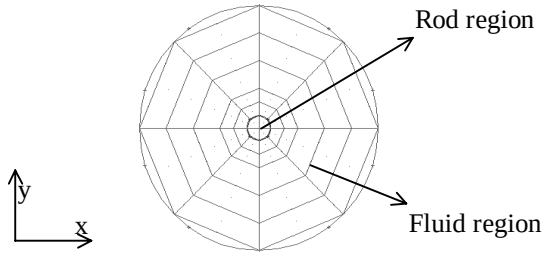

Figure 2 - Cross section mesh of the rod and fluid regions.

5. EXAMPLE 2: NATURAL FREQUENCIES AND PSD OF TWO RODS IN A FLUID

This case uses the data of Païdoussis *et al.* (1985) and the pre- and post-processing method of Section 3. In this reference, vibration analysis of clusters of two and three rods are performed. The excitation function was the PSD and CSD of the fluctuating pressure field on the rods. Just the two-rod system is going to be modeled using FEM/CFD. The two rods are coupled due to the fluid. The inflow velocity is modeled by a power law profile (Eq. (8)). The rods are simply supported. Their characteristics are presented in Païdoussis *et al.* (1985) using dimensionless parameters. These characteristics are specified in Table 3 such that these parameters are preserved, as dimension values must be used in the model.

Table 3. Characteristics of the rod, channel and fluid for example 2.

rod density ρ_{rod}	1137.2 kg/m^3
rod diameter $D_{rod}=2R_{rod}$	20 mm
rod length L	0.3334 m
rod inertia I	7853.98 mm^4
Young's module E	1.484 MPa
Poisson's ratio υ	0.47
smallest inter cylinder gap	10 mm
smallest cylinder to channel gap	56.4 mm
Channel diameter Dch	162.8 mm
fluid density ρ_{fluid}	996.4 kg/ m^3
fluid viscosity	9.541e-7 kg/(mm s)
fluid mean velocity V	1.157 m/s

5.1 Analytical value for the natural frequency of the rod in vacuum

The fundamental natural frequency of a simply supported rod in vacuum is given by Eq. (9). For a rod with the data shown in Table 3, this results in 16.04 rad/s or 2.55 Hz.

5.2 Determination of the natural frequency of the rod in vacuum (using FEM)

The natural frequency of the rod in vacuum was obtained using Spectrum code. The rod mesh has 99 nodes and 40 elements (10 longitudinal divisions) for each rod. The fundamental natural frequency obtained by Spectrum code is 15.25 rad/sec or 2.43 Hz (4.9% different from the analytical result). This result can be improved by refining the mesh but this would increase the computation time when working with the two-rods-fluid interaction. Due to computer limitations, this is not desirable and the result is considered satisfactory.

5.3 Determination of the natural frequencies and PSD of the rods in the fluid flow

The cross section meshes for the fluid and solid regions are shown in Fig. 3. The fluid mesh has 1342 nodes and 1060 elements. The fluid region is 1.5 times the length of the rod region, with the rod centered in it. The inlet fluid region length is divided in three parts. The mean fluid region length is divided in ten parts, following the rod division. The outlet fluid region length is divided in two parts. The rod mesh is the same of Section 5.2. The interface has 176 four nodded elements. The time dependent excitation forces were input in the central nodes of each longitudinal division of the rods. The boundary conditions for rods and fluid are the same of Section 4.3. The running time was about 40 hours on a HP-UX workstation.

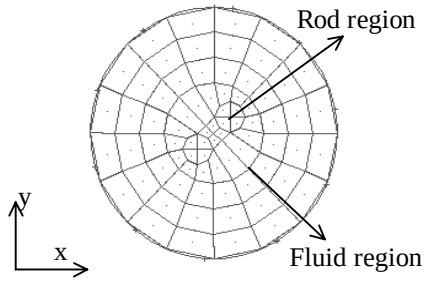

Figure 3 - Cross section of the fluid and of the two rods.

The pre-processing method for force sampling (Section 3.1) is used, with the following results:

- Pressure power and cross spectrum density:

Païdoussis *et al.* (1985) presented equations for the pressure PSD and CSD of a turbulent flow around a bundle of rods. The pressure PSD to be used here was derived from these equations using the data of Table 3. In order to simplify the sampling procedure, the axial correlation between the forces was neglected. This correlation is expected to be small as the longitudinal division of the rod mesh is relatively large. The resulting pressure PSD is:

$$S_{pp}(\omega)=\begin{cases}0.06157\exp(-0.004320\omega) & Pa^2s,\ \omega \geq 23.15\ rad/s\\ 0.002112\omega & Pa^2s,\ 0\leq\omega<23.15\ rad/s\end{cases}, \tag{10}$$

with ω *in rad/s*. The pressure CSD $S_{pp'}(\theta,\theta',\omega)$ is:

$$S_{pp'}(\theta,\theta',\omega)=\frac{S_{pp}(\omega)}{\left[1+0.2533S_\theta^2\right]\left[2-\exp\left\{-2.026S_\theta^2\right\}\right]}, \text{ and} \tag{11}$$

$$S_\theta=\begin{cases}\omega R_{rod}(\theta'-\theta)/V_c^\omega, & 0\leq|\theta'-\theta|<\pi\\ \omega R_{rod}[2\pi-(\theta'-\theta)]/V_c^\omega, & \pi\leq|\theta'-\theta|<2\pi\end{cases}, \tag{12}$$

where V_c^ω is the frequency dependent convective velocity at which the disturbances are transported dowstream, as defined by Bakewell (1968).

- Determination of the force power and cross spectral density $S_{f_if_j}(\omega)$:

The force PSD and CSD are determined by Eq. (1) to (3). The result of the numerical integration of these equations is shown in Fig. 4. The force PSDs $S_{f_xf_x}$ and $S_{f_yf_y}$ are equal, as expected. The cross spectral density $S_{f_xf_y}$ is negligible.

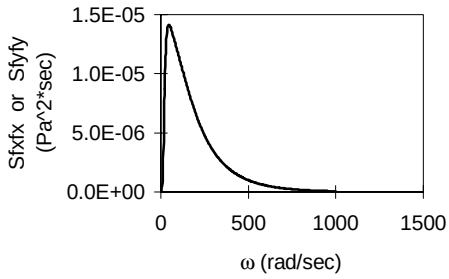

Figure 4 - Force Power Spectrum Densities $S_{f_x f_x}$ and $S_{f_y f_y}$ as a function of frequency ω

- Determination of the force cross correlation function:

The force cross correlation functions $R_{f_i f_j}(\tau)$ are equal to the covariance $\mathrm{cov}\left[f_i, f_j\right](\tau)$ as the mean value of the force distribution is zero. They are obtained using Eq. (5). By neglecting the axial dependence, this equation is reduced to (subscripts *i* and *j* can be *x* or *y*):

$$R_{f_i f_j}(\tau) = \mathrm{cov}\left[f_i, f_j\right](\tau) = \frac{1}{\pi}\int_0^\infty S_{f_i f_j}(\omega)\cos(\omega\tau)d\omega\,, \tag{13}$$

The variance of the *x* and *y* components of the force are equal. The covariance between *x* and *y* is negligible which means that the *x* and *y* force components are independent. The numerical integration was done from 0 to 1000rad/s and for 100 values of time increment τ (τ is multiple of the sampling time step). The sampling time step is 2.88e-2 s and is obtained by dividing the rod element length (33.34 mm) by the mean flow velocity (1.157 m/s). This time step is equivalent to a sampling frequency of 34.72 Hz. Thus, the covariance matrix terms are determined as a function of the time increments by Eq. (13). This covariance matrix is used in a Monte Carlo code in order to sample the values of the forces, as described in the next step.

- Sampling of the force in each rod central node position:

The nodal forces are sampled using a Monte Carlo procedure (Sbragio, 1998): the force covariance matrix is decomposed in two matrices using the Cholesky decomposition (Rabiner *et al.*, 1978). This decomposition expresses the covariance matrix as the product of a matrix by its transpose. For zero mean Gaussian distributions, the decomposed matrix can be used to transform the independent Gaussian samplings in a multivariate Gaussian distribution (Leon Garcia, 1994). The sampled forces are then applied to the central node of each section of the rod (except the end nodes, where no force is applied). Thus, for 10 divisions in each rod, 9 time-dependent forces in the *x* direction and 9 in the *y* direction are determined. The time dependence is obtained by sampling each force 100 times according to the time correlation previously determined. Hence, for two rods, a total of 36 independent multivariate Gaussian distributions with order 100 were sampled.

The displacement results from Spectrum code are submitted to a post-processing frequency domain analysis in order to obtain the natural frequencies and displacement PSD. Païdoussis *et al.* (1985) present two natural frequencies for each of the principal directions of movement (direction of the line that contains the rods, called radial direction and direction perpendicular to this line, called tangential direction). The total run time of the code was 3.772 s. This run time allowed to determine four natural frequencies, two for the radial direction displacements and two for the tangential direction displacements. The normalized PSDs of the displacements are shown in Fig. 5 and 6 and relates to the PSD by the following normalization formula:

$PSD_{normalized} = \left[\pi^2 / \left(4\varepsilon\beta^{1/2}u^3 k_2\right)\right] PSD$, where: (14)

$\varepsilon = L / D_{rod}$, (15)

$\beta = \rho_{fluid} / \left(\rho_{rod} + \rho_{fluid}\right)$, (16)

$u = \left(\rho_{fluid} A / EI\right)^{1/2} VL$, and (17)

$k_2 =$ constant = 2.0e-6. (18)

The parameters of these equations are shown in Table 3. Figure 5 shows the normalized displacement PSD in the radial direction while Fig. 6 shows in the tangential direction. The displacement PSDs determined in Païdoussis *et al.* (1985) are also shown for comparison.

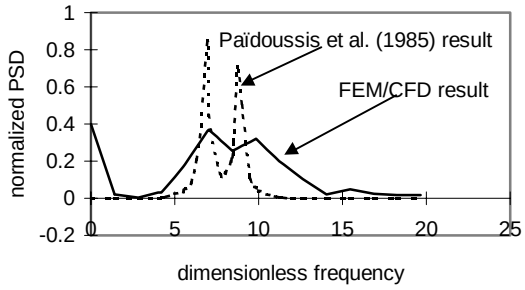

Figure 5 - Normalized displacement PSD in the radial direction.

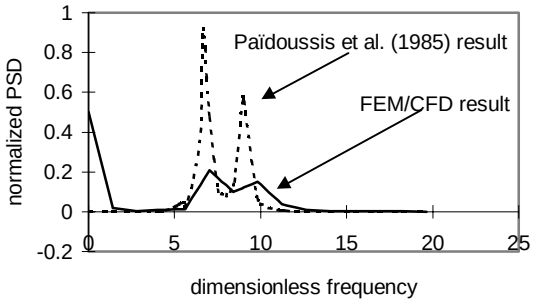

Figure 6 - Normalized displacement PSD in the tangential direction.

The natural frequencies are obtained from the peaks of the PSD graphs. The maximum time step used at the Spectrum solver was 0.004s. The total number of determined displacements was 943, covering a time history of the rod from 0s to 3.772s. According to Section 3.2, the frequency resolution for this case is 0.2651 Hz (1.666 rad/s) and frequencies are determined just in multiples of this value. If the difference between two natural frequencies is below this value, it is not possible to distinguish between them. A way to avoid this problem is increasing the number of sampled displacements which also increases the computation time.

The natural frequencies from Païdoussis *et al.* (1985) are presented as a dimensionless frequency ϖ which relates to circular frequency ω by the following normalization formula:

$$\omega = \frac{1}{L^2}\left[\frac{EI}{(m+\rho A)}\right]^{1/2} \varpi \cdot \tag{19}$$

From Païdoussis *et al.* (1985), the dimensionless natural frequencies for this system are:

- for movements in the radial direction: ϖ_2 = 6.95, and ϖ_3 = 8.73.

- for movements in the tangential direction: $\varpi_1 = 6.65$, and $\varpi_4 = 8.97$.

The dimensionless natural frequencies obtained from the FEM/CFD simulation are $\varpi_1 = \varpi_2 = 7.021$ (8.329 rad/s) and $\varpi_3 = \varpi_4 = 9.830$ (11.660 rad/s). These values are comparable to the natural frequencies of the system. It was not possible to distinguish between the results of the radial and tangential directions because of the frequency resolution. In this example, the error caused by the frequency resolution corresponds to a dimensionless value of 1.404 or 1.666 rad/s. This error is independent from the error due to the coarse mesh of the rod and fluid.

The natural frequency results from the FEM/CFD model are satisfactory in general but can be improved by decreasing the frequency resolution value. This can be done by increasing the number of displacement samples which increases the run time of the FEM/CFD solver.

6. CONCLUSION

This work presents a multiphysics simulation of rods in a fluid in order to determine their vibration behavior. The solver used is the Spectrum code which allows a simultaneous analysis of the fluid flow and rod movements by solving Navier Stokes and linear momentum equations.

Two examples are presented. The first example determines the natural frequencies of one rod in fluid flows of different velocities. The agreement between the Spectrum code results and the experimental data from Burgreen *et al.* (1958) was good even using a coarse mesh.

The second example determines the displacement PSD and natural frequencies of a system of two rods in a fluid. The forcing function used to excite the rod was obtained by integration of a pressure PSD function. The natural frequencies obtained in this example are quite satisfactory. However, some discrepancy in the displacement PSD intensity was noticed, probably due to the coarse mesh used. The forcing function used was taken from Païdoussis *et al.* (1985) and is probably the most difficult part of the modeling effort.

Hence, this work has established in a limited extent the feasibility of using random analysis and a commercial FEM/CFD code in order to study the complex problem of vibration of nuclear fuel rods. Multiphysics computation is an important tool in the simulation of this kind of problem as it allows the simultaneous solution of the vibration and flow problems.

REFERENCES

Bakewell Jr., H. P., 1968, Turbulent wall-pressure fluctuations on a body of revolution, The Journal of the Acoustical Society of America, Vol.43, number 6, pp.1358-1363.

Burgreen, D., Byrnes, J. J., and Benforado, D. M., 1958, Vibration of rods induced by water in parallel flow, Transactions of the ASME, Vol. 80, pp.991-1003.

Centric Engineering Systems Inc., 1993, Spectrum solver manuals, Version 1.0, May 1993.

Hinze, J. O., 1975, Turbulence, second edition, McGraw-Hill

Leon-Garcia, A., 1994, Probability and Random Processes for Electrical Engineering, 2nd edition, Addison-Wesley Publishing Company, Inc.

Païdoussis, M. P., and Curling, LL. R., 1985, An analytical model for vibration of clusters of flexible cylinders in turbulent axial flow, Journal of Sound and Vibration, V.98, n.4, pp.493-517.

Rabiner, L. R., and Schaefer, R. W., 1978, Digital processing of speech signals, Prentice Hall signal processing series.

Sbragio, R., 1998, The use of multiphysics computation in the determination of the vibration characteristics of nuclear fuel rods, Professional Degree Dissertation, Department of Nuclear Engineering and Radiological Sciences, The University of Michigan.